

RSC Advances



This is an *Accepted Manuscript*, which has been through the Royal Society of Chemistry peer review process and has been accepted for publication.

Accepted Manuscripts are published online shortly after acceptance, before technical editing, formatting and proof reading. Using this free service, authors can make their results available to the community, in citable form, before we publish the edited article. This *Accepted Manuscript* will be replaced by the edited, formatted and paginated article as soon as this is available.

You can find more information about *Accepted Manuscripts* in the [Information for Authors](#).

Please note that technical editing may introduce minor changes to the text and/or graphics, which may alter content. The journal's standard [Terms & Conditions](#) and the [Ethical guidelines](#) still apply. In no event shall the Royal Society of Chemistry be held responsible for any errors or omissions in this *Accepted Manuscript* or any consequences arising from the use of any information it contains.



Journal Name

ARTICLE

Molecular dynamics studies of interfacial crystallization behaviors in Polyethylene/carbon nanotubes composites

Bowen Yu,^a Sirui Fu,^a Zhiqiang Wu,^a Hongwei Bai,^a Nanying Ning,^b Qiang Fu^{*,a}Received 00th January 20xx,
Accepted 00th January 20xx

DOI: 10.1039/x0xx00000x

www.rsc.org/

Molecular dynamics simulations were utilized to study the interfacial crystallization between polyethylene (PE) and single walled carbon nanotubes (SWCNT). The early stage of PE crystallizing on the surface of SWCNT and SWCNT bundle were studied for comparison. The result showed that PE chain tended to stabilize in the grooves of SWCNT bundle and extended along the direction of SWCNT afterwards. The early arrived chain could then lead to a regular arrangement of other chains and this was conducive to the formation of interfacial crystallization. Also, the inner mechanism of interfacial crystallization in solution and melt had been investigated. It was found that in solution, the interfacial crystallization of PE is a spontaneous process. However, in melt the interfacial crystallization strongly depended on the pre-orientation of PE chains. This will help to understand the origin of polymer interfacial crystallization and guide for the fabrication of high performance polymer/CNTs nanocomposites via interfacial crystallization.

1. Introduction

Since discovered by Iijima in 1991,¹ carbon nanotubes (CNTs) have caused intensive concern in recent years owing to their great mechanical, electrical and thermal properties.²⁻⁶ These extraordinary properties make them ideal filler for preparing polymer composites.⁷⁻⁹ In order to achieve a great mechanical enhancement, strong interfacial adhesion between polymer matrix and CNTs is necessary because of its decisive role in load transfer.^{10,11} The interfacial enhancement can be realized by the following strategies: chemical modification of the CNTs to introduce various functional groups,^{12,13} in situ polymerization¹⁴ and non-covalent decorating of CNT surface using surfactant/ functionalized molecules^{15,16}. However, the chemical treatment to CNT could not be easily achieved and also changed the intrinsic properties of CNTs.¹⁷ Meanwhile, the non-covalent way was restricted to the weak interaction between coating molecules and CNTs. In recent years, interfacial crystallization is considered to be an efficient way to enhance the interfacial interaction between the two components since CNTs can act as an effective kind of nucleating agent for polymer crystallization.¹⁸⁻²⁰

To reveal the internal mechanism of interfacial crystallization,

molecular dynamics (MD) simulation has been considered as an efficient tool for investigating the intermolecular interactions between polymer chain and CNTs.²¹⁻²⁴ For example, Yongho Joo et al. compared two kinds of Conjugated polymers (PFO-BPy and PFO-BPy:Re) with different backbone rigidity. They found that the wrapping and unwrapping of the polymer chains can be greatly affected by the rigidity of polymer backbone.²⁵ By virtue of MD simulation, the adsorbing and ordering process of polymer molecules on CNTs can be observed visually thus a further understanding about the origin of interfacial crystallization will be obtained. Wei reported that the arrangement of PE chains strongly depended on the lattice structure of the SWCNT as well as the temperature.²⁶ Yang et al. focused on the crystallization process of single PE chains with different chain lengths on the SWCNT. They found that the attractive van der Waals interactions controlled the adsorption and pre-orientation of PE, and as the chain length of PE increased, more microstructures would appear in the final ordered structure.²⁷ Andrea Minoia and co-workers discussed more factors that might affect the interfacial interactions between PE and SWCNT, such as chirality, diameter, functionalization of SWCNT etc.²⁸ The results showed that the interface stability decreased with the curvature of the carbon surface, while the chemical groups present on SWCNT would hinder the regular arrangement of PE chain. However, these simulation results hardly considered the phenomena observed in experiment, and the mechanism of interfacial crystallization in actual processing still worth being further studied, since the formation of interfacial crystallization is a complicated process and will be affected by many factors. For example, Ning and

^a College of Polymer Science and Engineering, State Key Laboratory of Polymer Materials Engineering, Sichuan University, Chengdu 610065, China. Fax: 0086-28-85405402, Tel: 028-85405402, Email: qiangfu@scu.edu.cn.

^b State Key Laboratory of Organic-Inorganic Composites, Beijing University of Chemical Technology, Beijing 100029, China. Tel.: 86 10 64434860; Fax: 86 10 64433964. E-mail: ningny@mail.buct.edu.cn.

† Footnotes relating to the title and/or authors should appear here.

co-workers reported that nanohybrid shish kebab (NHSK) structure could be easily achieved using single-walled carbon nanotubes (SWCNT) bundles with “groove structure” on the surface.²⁹ It was found that the surface topography structure of CNTs was very important for the formation of NHSK. Additionally, the preparation methods also play a significant role in the formation of interfacial crystallization. Take the fabrication of polyethylene (PE) /CNTs composites as an example, NHSK structures can be obtained through the following means: solution crystallization¹⁸, solvent evaporation,³⁰ using supercritical CO₂ as antisolvent³¹ and also melt crystallization. The former three methods can be summarized as solution crystallization because they all take advantage of some kind of solvent. These solution crystallization methods hardly introduce any strong external field other than stirring. However, in melt crystallization process, the NHSK structures were prepared via dynamic packing injection molding technology (DPIM)³² or melt spinning³³. It is not hard to find that a strong shear or stretch field is necessary to form NHSK in melt crystallization. These external fields would impel the polymer chains to align along the direction of CNTs and this molecular orientation effect was conducive to the formation of interfacial crystallization. Limited by current characterization methods, the above-mentioned experiment observation cannot be explained intuitively and the internal mechanism of interfacial crystallization remains unclear. In this work, MD simulations were utilized to investigate the interfacial crystallization process of PE chains on SWCNT. The influence of SWCNTs' surface topography structure and different processing methods is examined. SWCNT and different kinds of SWCNT bundle were constructed for comparison study. It was found that the “grooves” on the surface of SWCNT bundle had a significant contribution to the stabilization and orientation of PE chain. Additionally, the difference between solution crystallization and melt crystallization was explored by varying the number of PE molecules, temperature as well as the orientation angles between PE molecules and SWCNT. The results are conducive to understand the origin of polymer interfacial crystallization and also offer an explanation to the unclear phenomena in experiment. Furthermore, guidance can be provided for the fabrication of high performance polymer/CNTs nanocomposites with NHSK.

2. Simulation Models and Methods

All the simulations in this work were performed using the Forcite module of Materials Studio developed by Accelrys Inc in the constant volume, constant temperature (NVT) ensemble. The Dreiding force field was chosen for its accuracy in investigating the mechanism of polymer crystallization.^{27, 34} The periodic boundary condition was not introduced.

2.1 Molecular Models

Since some of the factors that may influence the interfacial crystallization, such as the length of PE chain or the diameter and chirality of CNT have already been investigated,^{27, 28} all the

SWCNT and PE molecules used in the simulations are in the same size. The PE chain contained 100 repeat units. The SWCNT was (8, 8) armchair terminated by hydrogen atoms at both ends, with a diameter of 10.85 Å and a length of 196.76 Å. In the first part, initially, SWCNT bundle was constructed by arranging three SWCNTs (8, 8) in parallel and then the groove structure could be obtained. A schematic illustration of the construction process was shown in Figure 1. Firstly, a SWCNT was placed at a specified position. Then the SWCNT was moved right for a certain distance. After that, another SWCNT was put in the same position where the first one was located initially. This SWCNT was moved upper right for a same distance. Finally, the third SWCNT was placed at the initial position of the former two and a SWCNT bundle could be constructed. In order to minimize the strain energy, the SWCNT will not be rotated relative to one another. The distance between the two SWCNTs was 3.347 Å. The bundle was more stable at this distance because of the strong π - π stacking effect between the tubes. Since the conformation of SWCNT changed little during the simulation and this change would not influence the interactions between polymer chain and SWCNT,^{35, 36} both the SWCNT and SWCNT bundles were put along Z-axis and the position coordinates of all atoms was fixed to simplify the simulation procedure. In addition, to construct more different SWCNT bundles for comparison study, more different kinds of SWCNT bundles were constructed. On the one hand, the distance between the SWCNTs was gradually increased by 1 Å from 5 Å to 12 Å. On the other hand, three kinds of SWCNT bundles formed by different tubes were created. The combinations of SWCNTs were (20,20)/(20,20), (6,6)/(20,20), (11,0)/(6,6) and the distance between the two SWCNTs was 3.347 Å. In the second part, models with different number of PE molecules and different initial orientation angles were constructed. The SWCNT used in this part was (8, 8) armchair as well. The systems contained 1, 3, 10 PE chains respectively. The models with one PE chain are considered to represent the behavior in extremely dilute solution and the motion of PE chain is completely independent. In the models with more PE chains, entanglements between different chains will occur and can be considered as the behavior in melt. The initial orientation angles between PE and SWCNT varied from 0°, 45° to 90°. In actual processing, the introduction of external field can force the polymer chains to

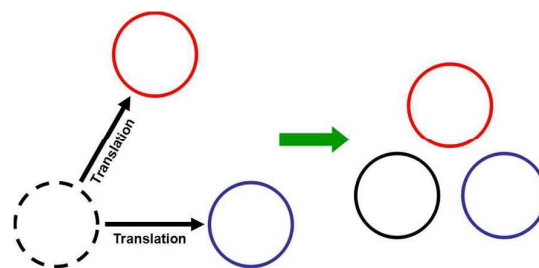


Fig. 1 Schematic illustration of the construction process for a SWCNT bundle (side view). Each circle represented a SWCNT.

align along a same direction. Therefore, the change of initial orientation angles is assumed to reflect the different external field condition. The parallel models represent the behavior of PE chains under a strong shear or stretch field. Thus there would be nine models in total.

2.2 Simulation Methods

The simulations could be divided into two parts. In the first part, the early stage of PE patterning on the surface of SWCNT and SWCNT bundle were studied for comparison. The initial conformations of the two models contained a SWCNT or SWCNT bundle respectively and a single PE chain which is close enough to absorb on the surface of SWCNT. The simulations were carried out at a temperature of 300 K under the control of Nose-Hoover thermostat. This temperature was much higher than the glass transition temperature (T_g) and would allow the conformation adjustment of PE chain on the SWCNT's surface. A time step of 1 fs and totally 5000 ps for the whole simulation process was used. The system could reach equilibrium after the entire simulation procedure.

In the second part, similar to the simulation in the first part, Nose-Hoover thermostat was employed to keep the temperature of the system constant. For the three systems that contained one PE chain, the simulation temperature was set to 300 K, below the melting temperature. These simulation procedures were corresponding to the interfacial crystallization process in solution. For the rest six systems that contained more PE chains, the simulations were performed at a relatively high temperature (700 K) for 200 ps to imitate the melting process. Longer simulations at 300 K would be carried out afterwards.

3. Results and discussion

3.1 Influence of SWCNT's topography structure

The conformation changes of PE chain on the surface of SWCNT are depicted in Figure 2. From this entire process, it is found that the interfacial crystallization behavior of PE can be divided to two stages, absorption and conformation adjustment. In the first stage, driven by the van der Waals interactions, the PE molecule will absorb and cover on the surface of SWCNT in a very short time (less than 100 ps). At this stage, the arrangement of PE segments is almost totally disordered. Then the conformation adjustment begins. The segments will realign on the surface of SWCNT trying to match the pattern of SWCNT and form a folded-chain crystal like

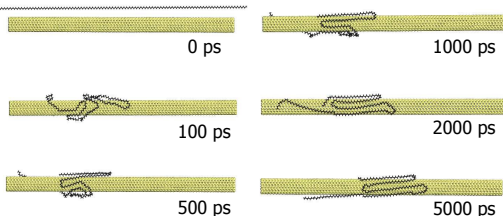


Fig. 2 MD snapshots of PE interacting with SWCNT at different time.

structure eventually (a visualized arrangement of the PE chain are shown in Figure 3). This is a time-consuming process and the final folded chain structure of PE chain still keeps sliding on the smooth surface of SWCNT and cannot stabilize at a certain position. At the same time, the orientation of folded chain structure is not completely along the direction of SWCNT. In Figure 3, a small angle between Z-axis and the direction of extended PE segments can be observed directly. This mismatch of orientation is apparently against the formation of interfacial crystallization in large-scale.

Next, the absorbing and ordering behavior of single PE chain on SWCNT bundle was investigated. In the fabrication of CNTs composites, the CNTs usually exist as ropes or bundles owing to the π - π interactions between each other. Therefore, groove structures will be formed between CNTs. In reality, a CNT bundle may contain several CNTs while in our simulation model, the CNT bundle was simplified as three SWCNT aligned in parallel. The reason of this simplification can be demonstrated as follow. The emphasis of our simulation is on exploring the influence of groove structures on PE crystallization, one groove is enough for a PE molecule to occupy and orient. Raising the number of SWCNTs to construct more grooves will not bring further results for single PE chain simulation. The conformation evolution of PE chain on the surface of SWCNT bundle was shown in Figure 4. Similar to the simulation in PE-SWCNT system, the PE chain absorb on the SWCNT bundle very shortly. The PE chain directly slides into the groove between two SWCNTs and stays there for the rest of simulation procedure. By comparing the conformations of PE at different time after 100 ps, it can be find that the conformations almost remain unchanged after the PE chain falls into the groove. This means that the groove structure is beneficial to the stabilization of PE and will greatly reduce the time of conformation adjustment. The time evolution of energy for PE-SWCNT and PE-SWCNT bundle is depicted in

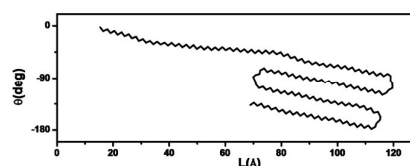


Fig. 3 2D profiles for the arrangement of carbon atom in PE chain. The L axis corresponds to the nanotubes long axis.

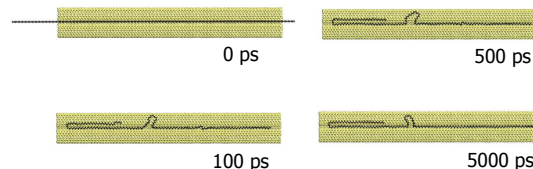


Fig. 4 MD snapshots of PE interacting with SWCNT bundle at different time.

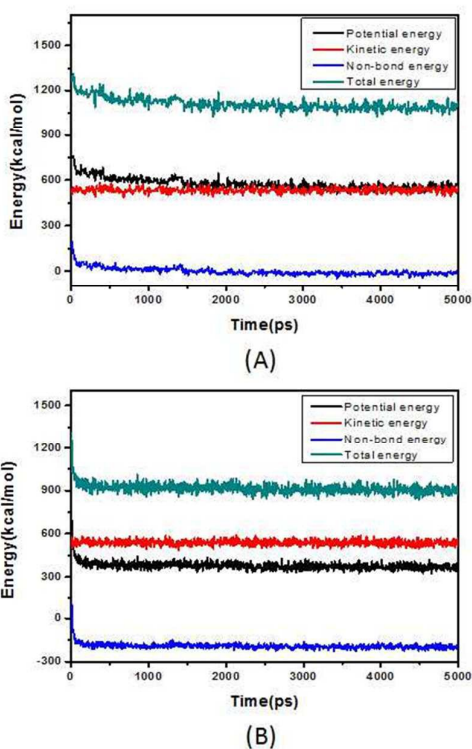


Fig. 5 Time evolution of energy for (A) PE/SWCNT and (B) PE/SWCNT bundle.

Figure 5. It takes less time for PE-SWCNT bundle to reach the equilibrium. To explore the origin of this difference, the interaction energy between PE and SWCNT/SWCNT bundle was calculated respectively using the following equation:

$$E_{\text{inter}} = E_{\text{total}} - E_{\text{polymer}} - E_{\text{SWCNT}}$$

In this equation, E_{inter} is the interaction energy between polymer molecule and the SWCNT, E_{total} is the total energy of the composite, E_{polymer} is the energy of individual polymer molecules and E_{SWCNT} is the energy of individual SWCNT or SWCNT bundle.²²⁻²⁴

The interaction energy between PE and single SWCNT is -296.8 kcal/mol, while the interaction energy between PE and SWCNT bundle is -503.5 kcal/mol. According to the energy minimization principle, PE chain will prefer to stay in the groove rather than other position on the surface of SWCNT. The great difference of interaction energy between the two systems can be explained by Figure 6. It is known that the PE chain interacts with the SWCNT mostly via CH- π interactions.³⁷ In Figure 6, a segment in PE chain is displayed as an example, on the surface of single SWCNT, only two hydrogen atoms of a segment are close enough to form CH- π interactions with the SWCNT. However, in the groove between two SWCNTs, the hydrogen atoms in PE will have more chances to form CH- π interactions with the SWCNT of both sides thus lead to enhancement of interfacial interaction.

Other than shortening the time of conformation adjustment, the groove structure formed by SWCNT bundles can also

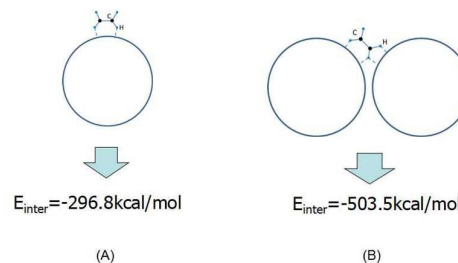


Fig. 6 Schematic representation of PE segment interacting with (A) SWCNT and (B) SWCNT bundle.

induce the PE chain to align along the direction of SWCNT axis. In the final snapshot of Figure 4, the PE chain expands in the groove and is basically parallel to the SWCNTs. The orientation of this early arrived PE chain can then lead to a regular arrangement of other chains. Further evidence is shown in Figure 7. This structure was obtained through the following way: The PE chains were introduced into the systems one by one, each time when a PE chain was introduced, a 1000 ps MD simulation procedure would be carried out under the same condition with single PE chain simulation. It is obvious that all the PE chains have significant orientation arrangement along the axis of SWCNT bundle, even those chains that were not close to the groove. Taking advantage of this uniform orientation of first arrived PE chains, the formation of interfacial crystallization will be achieved much easier.

There is also a fact that cannot be ignored in our simulation results. The PE chains on the surface of SWCNT bundles arrange as extended chain and barely fold. While in actual fabrication of NHSK, there was no apparent increase of the PE lamellae thickness when using SWCNT bundles instead of separate SWCNTs. A reasonable explanation is that, the results in the simulation only reflect the behavior of PE chains closest to the surface of SWCNT, which cannot be observed visually in experiment. Considering that most PE chains in lamellae are too far away from the SWCNT and the interactions between them are negligible. The entire crystallization process can be summarized as this. First, the PE chains wrap the SWCNT gradually and a monolayer of polymer is formed. Then the thin expanded PE layer on the surface of SWCNT just acts as nuclei to induce the homogeneous crystal growth of the outer PE chains. As a consequence, chain-folded lamellae structure will be formed rather than extended chain crystal. Further investigation will be carried out to confirm this. These

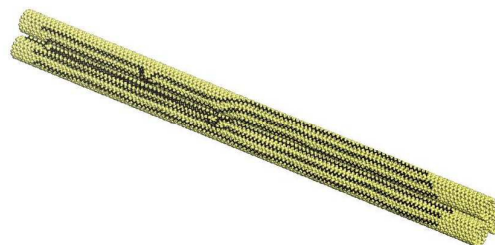
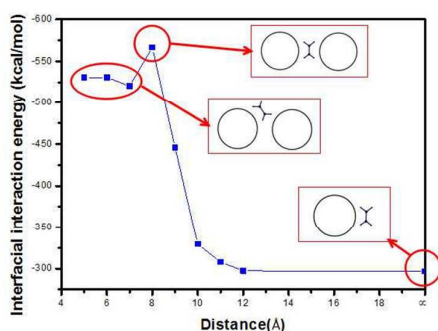
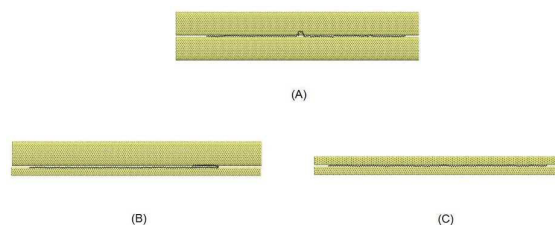


Fig. 7 More PE chains interacting with SWCNT bundle.

simulation results are consistent with the two-dimensional nucleation model in the formation of NHSK at early stage and can be considered as one more piece of evidence for this theory.

To further investigate the effect of groove in interfacial crystallization, different grooves were constructed in the following two ways: varying the distance between the SWCNTs and altering the composition of SWCNT bundle. MD simulations were carried out using the same method demonstrated previously and the interaction energy between PE and SWCNT bundles were calculated respectively. The relationship between the separation distance and the interaction energy are shown in Figure 8. It can be found that when the separation distance is smaller than 7 Å, the interaction energy between PE and SWCNT bundles will remain about the same. This indicates that the orientation of the PE chain can be induced by the bundles efficiently. When the separation distance between SWCNTs becomes 8 Å, the strongest interfacial interaction energy will be observed. With further increase of the separation distance, the interaction energy decreases rapidly and finally approaches the value of single SWCNT/PE interaction. This can be explained by the three schemes in Figure 8. With separation distance smaller than 7 Å, the PE chain will fall into the groove to form more CH- π interactions with the SWCNT as demonstrated in previous section (Figure 6-B). When the separation distance is 8 Å, the PE chain will exactly stay between the two SWCNTs and in this case, the most CH- π interactions will be formed and lead to the strongest interfacial interaction. With greater separation distance, the PE chain cannot have strong interactions with both of the SWCNTs and no favorable conformation along the SWCNT's long axis can be achieved, thus the orientation induced by the groove is weak. As a consequence, only tight SWCNT bundles can have a significant contribution to the stabilization and orientation of PE chain. Next, three kinds of SWCNT bundles formed by different tubes were created as demonstrated before. The final conformations of the three structures are shown in Figure 9. In all three systems, the PE chains are aligned along the groove without

**Fig. 8** Evolution of interfacial interaction energy with the change of separation distance between SWCNTs**Fig. 9** Final conformations of single PE chain interacting with different SWCNT bundle, (A) (20,20)/(20,20), (B) (20,20)/(8,8) and (C) (11,0)/(6,6).

exception. The interaction energy obtained is -586.0 kcal/mol, -579.7 kJ/mol and -560.3 kJ/mol respectively, suggesting a strong interfacial adhesion for all the three structures. This means that bundles formed by SWCNTs with different diameters and chirality can all lead to a regular alignment of the PE chain.

3.2 Influence of processing method and pre-orientation

Models that contained one PE chain and one SWCNT were constructed to reflect the crystallization behaviors in solution. This is because in solution, the concentration of polymer molecules is very low. At the early stage of interfacial crystallization, the behavior of a polymer chain can be considered to be independent. Thus the interaction between polymer chains and SWCNT can be simplified. The initial and final conformations of the three models are shown in Figure 10. Folded chain structures can be observed in all three models, and these final folded chain structures do not show anything particular in the orientation of chains. This means that the ordering arrangement of PE chain on the surface of SWCNT is inherent. Whatever the initial condition of orientation is, the PE chain will form a folded chain structure approximately along the direction of SWCNT's long axis. This can be a good explanation for the mechanism of interfacial crystallization formed in solution. The spontaneous ordering of PE chain on the SWCNT's surface will lead to the formation of interfacial crystallization. Pre-orientation is unnecessary thus no external field is needed in solution. Additionally, crosses between two segments of the polymer chain can be observed in the latter

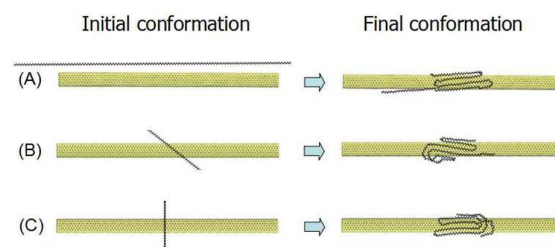


Fig. 10 MD simulation snapshots of the initial conformations and final conformations for single PE chain interaction with different orientation angle, (A) 0°, (B) 45°, (C) 90°.

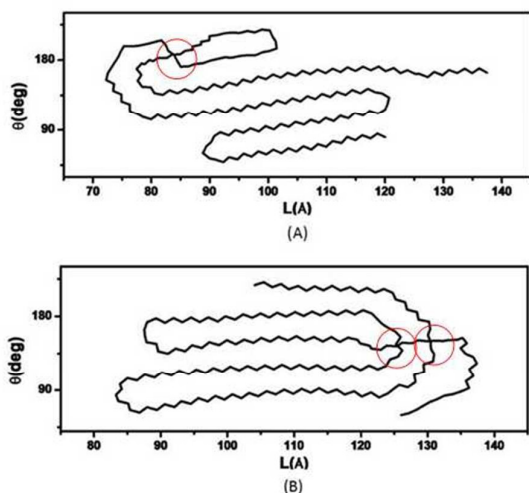


Fig. 11 2D profiles for the PE chain interaction with different orientation angle, (A) 45°, (B) 90°.

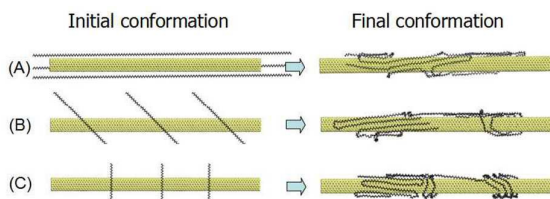


Fig. 12 MD simulation snapshots of the initial conformations and final conformations for 3 PE chains interaction with different orientation angle (A) 0°, (B) 45°, (C) 90°.

two models. It is more intuitive in 2D-profile of the polymer chains (highlighted by the circles in Figure 11-A and B). It is found that these crosses, once formed, cannot be eliminated by the conformation adjustment. These crosses may lead to defects in the formation of interfacial crystallization. The initial and final structures of the three models that contain 3 PE chains, representing a transition between solution and melt, are shown in Figure 12. Compared with the results in single chain simulation part, it is obvious that the arrangement of PE segments is less regular. Detail information of the arrangement can be revealed by the 2D-profile shown in Figure 13. Folded chain structures can be observed in all three models (highlighted by purple ellipses) and these structures can be formed both by one chain (Figure 13-C) or several different chains (Figure 13-A and B). In Figure 13-A, most of the segments in PE chains are extended along the long axis of

SWCNT and barely wrap around the SWCNT. While in Figure 13-B and C, the PE chains wrap around the SWCNT to varying degrees. It shows a great difference from the results in single

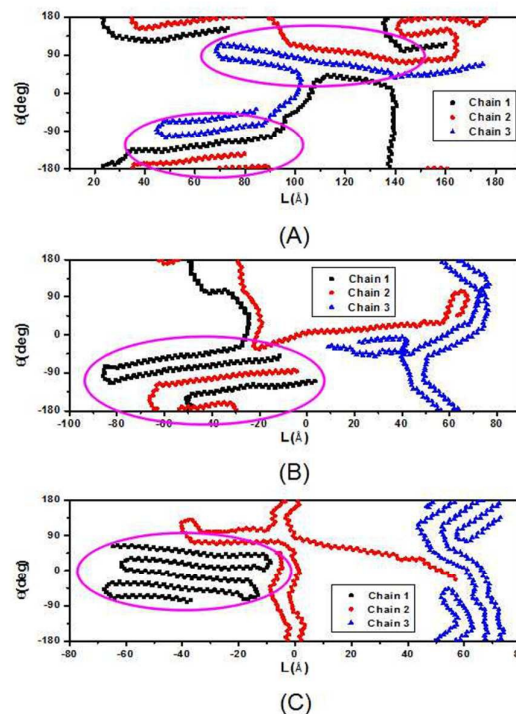


Fig. 13 2D profiles for the 3 PE chains interaction with different orientation angle, (A) 0°, (B) 45°, (C) 90°.

chain simulations. This means that the initial orientation angle of PE chains will affect the formation of interfacial crystallization to a certain extent. It can be explained as following. Originally, at the absorption stage, the PE chains with a large initial angle have more chance to wrap around the SWCNT. In the following conformation adjustment stage, if the motion of segments is totally free, the wrapping part of PE chain can be eliminated gradually and a superior folded chain structure will be formed eventually. On the other hand, if there are more PE chains absorbed on the surface of SWCNT at the same time, the motion of segments will be hindered by other chains and the wrapping structures have to be maintained. Therefore, a pre-orientation of PE chains and SWCNT is favorable for the formation of interfacial crystallization.

Finally, the early stage of interfacial crystallization in melt was investigated by adding more PE chains that could cover the SWCNT surface completely. As demonstrated in the part of Simulation Method, the simulations were initially performed at 700 K (above the melting temperature) for 200 ps to imitate the melting process. Then the ordering behavior of PE chains was examined under a longer simulation time at 300 K. The conformations of the three models at different stage were

shown in figure 14. After the melting process, the PE chains in all three models distribute loosely around the SWCNT and form a thin layer. At this high simulation temperature, owing to the high mobility of polymer chains, the segments will keep moving and no regular structures will be formed. By comparing the three conformations after melting with different initial orientation angles, it can be found that the PE chains in Figure 14-A are mainly extended along the long axis of SWCNT, showing a pre-orientation effect. While for the rest two models in which the PE chains were not arranged parallel to the SWCNT initially, the distribution of PE chains is almost entirely random. Meanwhile, the SWCNT is not covered completely and some part of the surface is bare. After the following crystallizing process, the cover of PE chains become tighter and the SWCNT are fully coated by the PE chains. The final conformation in Figure 14-A still shows an obvious difference from the latter two. Likewise, the 2D-profile of the three structures is drawn to analyze in detail (shown in figure 15). In figure 15-A, most of the PE chains are approximately parallel and an extended chain-like structure can be observed. These uniformly arranged PE chains can act as nuclei to induce the homogeneous crystal growth of the outer PE chains. In Figure 15-B and C, although local folded chain-like structure can be observed, the orientation of these structures is variance. Therefore, it is impossible to form a large scale interfacial crystallization on this occasion. Cylindrical distribution functions of the hydrogen atoms and carbon atoms in PE chains are shown in Figure 16-A. It can be found that the peak of C atoms represented for the parallel model is higher than the rest, also implying a more regular distribution

of polymer chains on the surface of SWCNT. To rationalize the mechanism of this distinction, bond-orientational order parameter A was calculated which is defined as follows:

$$A = \frac{1}{n-2} \sum_{i=3}^n \left(\frac{3 \cos^2 \psi_i - 1}{2} \right),$$

where n is the number of CH_x per PE chain, ψ_i is the angle between the vector b_i of the smallest segment and Z-axis. The value range of the order parameter is $[-0.5, 1]$, indicating a different degree of orientation. The value of -0.5 and 1 correspond to the chain perfectly perpendicular or parallel to the Z-axis respectively. A detail definition of parameter A can be inspired by the nematic liquid-crystal order parameter.³⁸ Figure 16-B shows evolution of order parameter as a function of time. In all three models, the values of A increase initially and tend to flatten at last. The final value of the parallel model, which is 0.65 , is significantly higher than the 45° and 90° models (0.38 and 0.31 , respectively), indicating a better orientation effect. The gently change of order parameter suggests that once the SWCNT is entirely covered by PE chains, there will be little space for conformation adjustment of segments. Due to the restriction of the neighboring segments, the conformation adjustment can only occur in a small range. As a result, the pre-orientation of PE chains in melt crystallization is extremely important for the formation of large scale interfacial crystallization. In order to explore the interfacial enhancement caused by interfacial crystallization, the interaction energy between SWCNT and PE matrix is

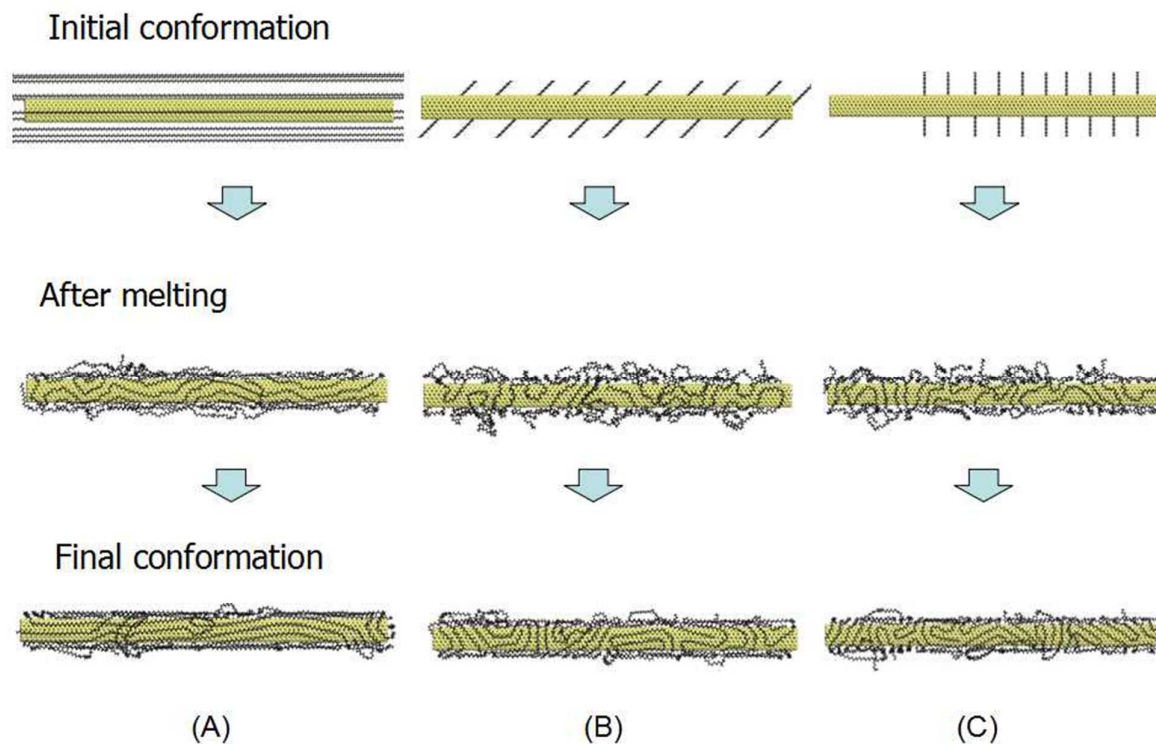


Fig. 14 MD simulation snapshots of the initial conformations, melting conformations and final conformations for 10 PE chains interaction with different orientation angle (A) 0°, (B) 45°, (C) 90°.

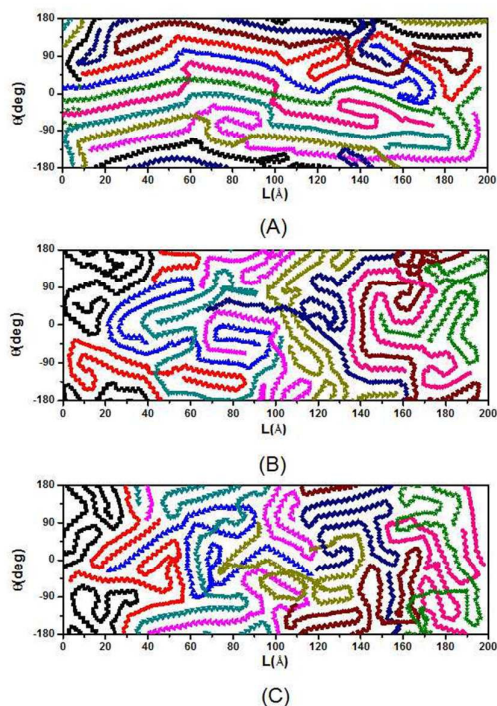


Fig. 15 2D profiles for the 10 PE chains interaction with different orientation angle, (A) 0°, (B) 45°, (C) 90°.

using equation (1). The value of interaction energy for the three different initial orientation angle is -2487.3 (0°), -2311.3 (45°) and -2274.7 (90°) kcal/mol respectively. It implies that interfacial crystallization will improve the interfacial adhesion between the PE matrix and SWCNT. This is because a more regular arrangement of PE chains leads to a narrow distribution of hydrogen atoms. As shown in Figure 16-A, there are more hydrogen atoms in parallel model that are close to the surface of SWCNT. Hence more CH- π interactions can be formed and enhance the interfacial adhesion eventually.

Conclusions

In this work, MD simulations were employed to investigate the interfacial crystallization behavior of PE chains on the surface of SWCNT. The simulation results shows that, groove structure formed by tight SWCNTs bundle is beneficial to the orientation of PE chain due to the stronger interfacial interaction between PE and SWCNT in the groove. The combinations of the bundles have no effect on the orientation. In addition, in solution crystallization, the ordering arrangement of PE chain on the surface of SWCNT is initiative thus the pre-orientation of the PE chain is not necessary. While in melt crystallization, when the SWCNT is fully covered by PE chains, the conformation adjustment is insufficient and only if a pre-orientation of the

PE chains along the direction of SWCNT's long axis are introduced, a regular interfacial crystallization structure can be obtained. Meanwhile, the formation of interfacial

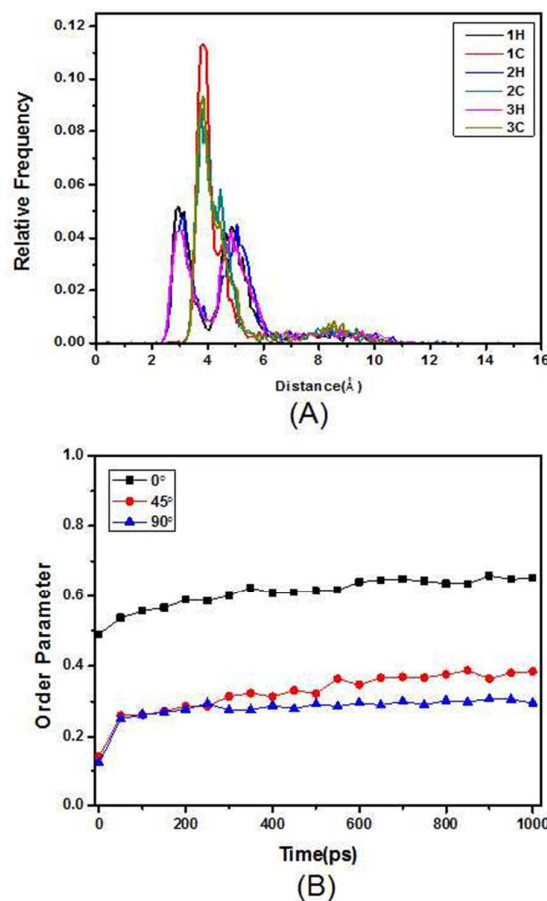


Fig. 16 (A) Cylindrical distribution functions of the hydrogen atoms and carbon atoms in PE chains, and (B) time evolution of the order parameter A of 10 PE chains on the SWCNT.

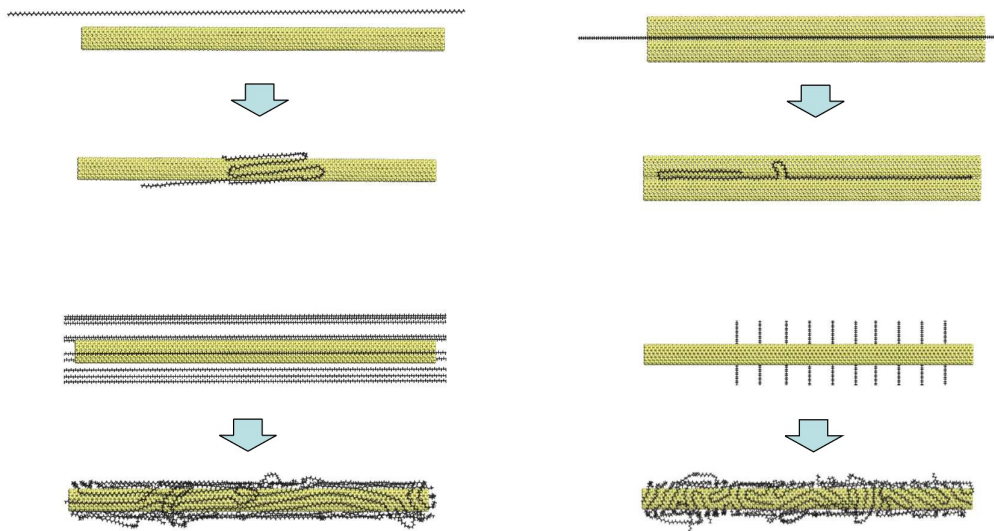
crystallization will lead to enhancement of the interfacial adhesion. In future, we will try to construct models with randomly distributed PE chains around the SWCNT and introduce some shear stress for further study.

Acknowledgement

We gratefully acknowledge the financial support from the National Natural Science Foundation of China (51421061 and 51210005) and State Key Laboratory of Organic-Inorganic Composites, Beijing University of Chemical Technology, which provided the Materials studio software.

Notes and references

- 1 S. Iijima and T. Ichihashi, 1993.
- 2 E. W. Wong, P. E. Sheehan and C. M. Lieber, *Science*, 1997, **277**, 1971-1975.
- 3 T. W. Odom, J.-L. Huang, P. Kim and C. M. Lieber, *Nature*, 1998, **391**, 62-64.
- 4 T.-Y. Choi, D. Poulidakos, J. Tharian and U. Sennhauser, *Nano letters*, 2006, **6**, 1589-1593.
- 5 T. Li, J.-H. Pu, L.-F. Ma, R.-Y. Bao, G.-Q. Qi, W. Yang, B.-H. Xie and M.-B. Yang, *Polymer Chemistry*, 2015, DOI: 10.1039/C5PY01236H.
- 6 S. Pande, A. Chaudhary, D. Patel, B. P. Singh and R. B. Mathur, *RSC Advances*, 2014, **4**, 13839.
- 7 J. N. Coleman, U. Khan, W. J. Blau and Y. K. Gun'ko, *Carbon*, 2006, **44**, 1624-1652.
- 8 M. Cadek, J. N. Coleman, K. P. Ryan, V. Nicolosi, G. Bister, A. Fonseca, J. B. Nagy, K. Szostak, F. Beguin and W. J. Blau, *Nano Letters*, 2004, **4**, 353-356.
- 9 P. Bilalis, D. Katsigiannopoulos, A. Avgeropoulos and G. Sakellariou, *RSC Advances*, 2014, **4**, 2911.
- 10 N. Ning, S. Fu, W. Zhang, F. Chen, K. Wang, H. Deng, Q. Zhang and Q. Fu, *Progress in polymer science*, 2012, **37**, 1425-1455.
- 11 J. N. Coleman, U. Khan and Y. K. Gun'ko, *Advanced materials*, 2006, **18**, 689-706.
- 12 B. X. Yang, K. P. Pramoda, G. Q. Xu and S. H. Goh, *Advanced Functional Materials*, 2007, **17**, 2062-2069.
- 13 F. H. Gojny and K. Schulte, *Composites Science and Technology*, 2004, **64**, 2303-2308.
- 14 C. Park, Z. Ounaies, K. A. Watson, R. E. Crooks, J. Smith, S. E. Lowther, J. W. Connell, E. J. Siochi, J. S. Harrison and T. L. St Clair, *Chemical physics letters*, 2002, **364**, 303-308.
- 15 A. Star, J. F. Stoddart, D. Steuerman, M. Diehl, A. Boukai, E. W. Wong, X. Yang, S. W. Chung, H. Choi and J. R. Heath, *Angewandte Chemie International Edition*, 2001, **40**, 1721-1725.
- 16 A. Star, Y. Liu, K. Grant, L. Ridvan, J. F. Stoddart, D. W. Steuerman, M. R. Diehl, A. Boukai and J. R. Heath, *Macromolecules*, 2003, **36**, 553-560.
- 17 D. Tuncel, *Nanoscale*, 2011, **3**, 3545-3554.
- 18 L. Li, C. Y. Li and C. Ni, *Journal of the American Chemical Society*, 2006, **128**, 1692-1699.
- 19 A. R. Bhattacharyya, T. V. Sreekumar, T. Liu, S. Kumar, L. M. Ericson, R. H. Hauge and R. E. Smalley, *Polymer*, 2003, **44**, 2373-2377.
- 20 E. D. Laird and C. Y. Li, *Macromolecules*, 2013, **46**, 2877-2891.
- 21 K. Liao and S. Li, *Applied Physics Letters*, 2001, **79**, 4225-4227.
- 22 S. S. Tallury and M. A. Pasquinnelli, *The Journal of Physical Chemistry B*, 2010, **114**, 4122-4129.
- 23 Q. Zheng, Q. Xue, K. Yan, L. Hao, Q. Li and X. Gao, *The Journal of Physical Chemistry C*, 2007, **111**, 4628-4635.
- 24 M. Shan, Q. Xue, T. Lei, W. Xing and Z. Yan, *The Journal of Physical Chemistry C*, 2013, **117**, 16248-16255.
- 25 Y. Joo, G. J. Brady, M. J. Shea, M. B. Oviedo, C. Kanimozhi, S. K. Schmitt, B. M. Wong, M. S. Arnold and P. Gopalan, *ACS nano*, 2015.
- 26 C. Wei, *Nano letters*, 2006, **6**, 1627-1631.
- 27 H. Yang, Y. Chen, Y. Liu, W. S. Cai and Z. S. Li, *The Journal of chemical physics*, 2007, **127**, 094902.
- 28 A. Minoia, L. Chen, D. Beljonne and R. Lazzaroni, *Polymer*, 2012, **53**, 5480-5490.
- 29 N. Ning, W. Zhang, Y. Zhao, C. Tang, M. Yang and Q. Fu, *Polymer*, 2012, **53**, 4553-4559.
- 30 L. Li, W. Wang, E. D. Laird, C. Y. Li, M. Defaux and D. A. Ivanov, *Polymer*, 2011, **52**, 3633-3638.
- 31 J. Yue, Q. Xu, Z. Zhang and Z. Chen, *Macromolecules*, 2007, **40**, 8821-8826.
- 32 J. Yang, C. Wang, K. Wang, Q. Zhang, F. Chen, R. Du and Q. Fu, *Macromolecules*, 2009, **42**, 7016-7023.
- 33 F. Mai, K. Wang, M. Yao, H. Deng, F. Chen and Q. Fu, *The Journal of Physical Chemistry B*, 2010, **114**, 10693-10702.
- 34 Y.-K. Lan and A.-C. Su, *Macromolecules*, 2010, **43**, 7908-7912.
- 35 H. Chen, Q. Xue, Q. Zheng, J. Xie and K. Yan, *The Journal of Physical Chemistry C*, 2008, **112**, 16514-16520.
- 36 M. Yang, V. Koutsos and M. Zaiser, *The Journal of Physical Chemistry B*, 2005, **109**, 10009-10014.
- 37 D. Baskaran, J. W. Mays and M. S. Bratcher, *Chemistry of Materials*, 2005, **17**, 3389-3397.
- 38 J. Prost, *The physics of liquid crystals*, Oxford university press, 1995.



The interfacial crystallization of polyethylene can be greatly affected by the SWCNT's surface topography and pre-orientation of polyethylene chains